



HAL
open science

Large scale rainfall simulation to investigate infiltration processes in a small landslide under dry initial conditions: the Draix hillslope experiment

E. Garel, V. Marc, S. Ruy, A.-L. Cognard-Plancq, S. Klotz, C. Emblanch, R. Simler

► To cite this version:

E. Garel, V. Marc, S. Ruy, A.-L. Cognard-Plancq, S. Klotz, et al.. Large scale rainfall simulation to investigate infiltration processes in a small landslide under dry initial conditions: the Draix hillslope experiment. *Hydrological Processes*, 2012, 26 (14), pp.2171-2186. 10.1002/hyp.9273 . hal-02294345

HAL Id: hal-02294345

<https://hal.science/hal-02294345>

Submitted on 2 Oct 2023

HAL is a multi-disciplinary open access archive for the deposit and dissemination of scientific research documents, whether they are published or not. The documents may come from teaching and research institutions in France or abroad, or from public or private research centers.

L'archive ouverte pluridisciplinaire **HAL**, est destinée au dépôt et à la diffusion de documents scientifiques de niveau recherche, publiés ou non, émanant des établissements d'enseignement et de recherche français ou étrangers, des laboratoires publics ou privés.

Large scale rainfall simulation to investigate infiltration processes in a small landslide under dry initial conditions: the Draix hillslope experiment

E. Garel¹, V. Marc¹, S. Ruy², A.-L. Cognard-Plancq¹, S. Klotz³, C. Emblanch¹, Simler, R¹.

¹ Université d'Avignon et des Pays de Vaucluse, UMR EMMAH 1114 INRA-UAPV, 33 rue Louis Pasteur, 84000 Avignon, France.

² Institut National de la Recherche Agronomique, UMR EMMAH 1114 INRA-UAPV, Domaine Saint-Paul 84914 Avignon Cedex 9, France.

³ Cemagref Grenoble, ETNA, 38402 Saint Martin d'Hères BP 76, France.

Abstract

Few studies exist on infiltration processes in badlands, although infiltration and subsurface lateral flows are known to contribute to soil erosion and to control slope instability. Our investigation was carried out in a 100 m² plot located in a 0.5 ha landslide in black marls (South-East France). An artificial sprinkling was performed with an intensity of 10 mm.h⁻¹ during 66.4 h interrupted with 8.4 h. breaks. KBr and KCl were used as tracers.

A pseudo-steady state was reached after 25-35 hours and 250-350 mm of rainfall. The runoff coefficient was 40% (ratio total runoff volume/total sprinkling water amount). Pre-event water (PE) contributed to the groundwater recharge at the very beginning of the experiment but PE contribution dropped steadily while the soil was saturating. After around 200 mm cumulative rainfall, PE contribution started to rise steeply before reaching a nearly constant value. This original mechanism implies an efficient transfer process of PE. It was assumed from the description of the material structure and from hydrological evidences that PE was mainly drained from a structure porosity made of the marl's flaked nature. Total pre-event water contributions ranged from 25 to 79 % (PE contribution was over 50 % in 2/3 of the observations wells). Over the recession phase, release of pre-event water occurred from the drainage of a texture porosity. The study showed that at the plot scale, infiltration processes proved well organised despite the high heterogeneity and anisotropy of the material. It was possible to propose a general conceptual model explaining the hydrological processes over time and area. The peculiar structure of regolith originating from black marl is preserved over a large part of the weathering time, so that the material structure (type, orientation of grains, small/large pores) remains a first order control of water flow generation in Black marl soils.

Key words: Hillslope hydrology, Artificial tracing, Sprinkling experiment, Infiltration, French South Alps, Landslide,

Introduction

In mountainous areas and especially in badland context, infiltration processes and water storage are known to play a key role in the slope stability (by enhancing pore water pressure) and in the soil erosion (Antoine et al., 1995 ; Bryan and Jones, 1997; Lorente et al. 2002; Descroix and Mathys, 2003; Griffiths et al., 2005). Surprisingly, most studies on hydrological processes in badlands have been focused on Hortonian runoff processes (Araguàs Catchment: Nadal-Romero and Regues, 2009; Vallcebre Catchment: Gallart et al. 1997; Regues and Gallart, 2004; Latron and Gallart, 2008, Tabernas Catchment: Cantón et al., 2001; Canton et al., 2004; Li et al., 2005; Draix catchment: Wijdenes and Ergenzinger, 1998; Lukey et al. 2000; Mathys et al., 2003; Mathys et al., 2005; Biancana Badland: Torri et al., 1994; Torri et al., 1999). Subsurface processes have traditionally been regarded as of minor importance compared to surface flows for discharge production and soil erosion (Maneta et al., 2008) and infiltration processes have not been much investigated. Nevertheless, in such environments, some of these studies have shown that very low values of discharge coefficients (Cantón et al., 2001; Regues and Gallart, 2004; Nadal-Romero et al., 2008; Mathys et al., 2005) and very high hydraulic conductivity of soils (Li et al., 2005; Esteves et al. 2005) could be observed. For these reasons, the exact role of subsurface processes in badland context needs to be clarified.

The aim of the present study was to investigate the hillslope subsurface hydrology of an active landslide consisting of black marl. The experimental basins of Draix have been monitored since 1984 to study erosion and flash flood generation in Black marl badlands (Richard and Mathys, 1999). Hydrological investigations were undertaken at the plot scale (Mathys et al., 2005) as well as at the catchment scale (Lukey et al., 2000; Cras et al., 2007). Cras et al. (2007) partly elucidated the role of subsurface flow and the contribution of pre-event water at the hillslope and catchment scales. In the present study, a large scale artificial sprinkling experiment was carried out in a small 100 m² landslide. Different artificial tracers were successively applied to assess the impact of initial soil moisture conditions. In detail, this work aimed at (1) establishing the conditions for preferential flows initiation (soil surface conditions, slope variation, initial soil moisture), (2) identifying the interaction between the different structural soil units and quantifying the mixing processes with pre event water, and (3) proposing a general concept for the hillslope hydrological functioning.

1. Study site presentation

The study site is a small 0.5 ha translational rock block landslide (figure 1). The landslide is limited downslope by the Laval torrent. Geotechnical and geophysical investigations have been carried out at the site since its triggering in winter 1998 to observe its internal structure and the subsurface topography (Malet, 2003; Fressard, 2008; Grandjean et al., 2009). This site provides the opportunity to study a small landslide evolution since the exact time of its initiation.

The experimental plot was situated in the lower part of the slope (Fressard, 2008). The 100 m² plot was rectangular, 7 m large and 14 m long. The mean elevation was 884.5 m. The surface

slope was 50 % in the upper part of the plot and dropped to 28 % downwards. The depth of regolith was estimated to 4 m in the upper part of the plot and 5 m downslope. The substratum is made of fresh, non weathered black marl.

2. Regolith and block properties

The landslide is made of marl blocks 0.1 m to 1 m size, wrapped into a formation of reworked marl made of flakes (1 mm to several cm long) or of a clayey matrix (deeper zones). The laminated structure of the marl is well observed in the blocks, either weathering or still compact. The random distribution of the blocks and hence the variable direction of the stratification joints resulted in a highly disorganised medium. Accordingly, several preferential water flow pathways are observed: large macropores made by the blocks layout (hollows only partly filled by reworked material) and openings between marl layers due to the decompression of blocks (figure 2).

Porosities were measured at the laboratory from 1240 cm³ samples (steel cylinders of 150 mm diameter and 70 mm height) of reworked marl and small blocks. Material samples were taken from calibrated stainless steel rings. For each sample, the total porosity was obtained from the bulk density measurements. The porosity of reworked marl ranged from 0.38 to 0.53 whereas the values obtained for the blocks ranged from 0.17 to 0.42.

The saturated hydraulic conductivity was measured in the field with a suction permeameter and using slug tests methods. Results proved very different according to area owing to the heterogeneity and anisotropy of the medium (blocks within the matrix, different behaviour according to the direction of stratification). Results from the suction permeameter were in a range of 10-180 mm/h in agreement with the results by Esteves et al. (2005) (20-230 mm/h).

3. Methods

Rainfall intensity, evaporation rate, soil moisture, surface runoff and groundwater level were monitored all over the experiment (figure 3). Observation wells were also used for water sampling. At last, geophysical techniques were applied to make an areal investigation of infiltration processes (Travelletti et al., 2011)

3.1. Rainfall and evaporation monitoring

The rainfall simulation was carried out using 6 sprinklers spread around the plot. Rainfall amount was measured every 2 hours from 12 rain gauges distributed all over the plot. Time series at shorter time steps were available from an automatic rainfall recorder set up at the middle of the plot.

The evaporation measurements were done using microlysimeters (Boast and Robertson, 1982). The microlysimeters were made from PVC cylinders pushed to the soil, removed with

the soil inside and then closed from the bottom with the plastic cup to prevent soil and water exchange. Then they were weighed and replaced into the soil. 24 hours later, microlysimeters were weighed again.

3.2. Piezometers locations and monitoring

28 open standpipe piezometers 0.77 m to 3.87 m deep were used to study the areal and time variation of groundwater head. They were set up according to 3 transects perpendicular to the main surface slope ((aa'); (bb') and (cc')). 6 additional boreholes were drilled outside, below the plot (dd'). 4 piezometers drilled in February 2007 (AC, AE, CA, CH) were equipped with a 1 m long screen and were closed at the bottom. The other observation wells were made 24 h to 48 h before the experiment. They were open at the bottom and had 50 cm long screens. The annular space between the drilled hole and the PVC pipe was filled with gravels and then sealed with bentonite clay to prevent any preferential flow along the tube. As much as possible, these piezometers were distributed according to groups of 2 or 3, set up side by side at different depths. The upper part of the rainfall simulation area was devoid of piezometers owing to the steep slope (50 %). Piezometers AA, AB, AC, BC, BD, CF, CG and CH, situated on the steepest gradient line, were equipped with Paratronic® CNR water level recorders (accuracy 0.1 % full scale for 1 m max variation). The recording time step was 30 min. Piezometers BG, CH and AE were equipped of Diver® water level recorders (accuracy 0.05% full scale). Capillary tubes devoted to water hand-sampling were inserted into each piezometer.

Of the 28 piezometers, only 11 were subjected to water level variations during the experiment. Moreover, for technical reasons, some piezometers were not used for sampling although a water level variation was observed (i.e. Piezometer CH). Finally, water was sampled in 9 piezometers (figure 4 and table 1).

3.3. Soil moisture measurements

12 TDR probes 20 cm long (TRASE datalogger and multiplexer) were used to investigate the soil moisture variation with depth along a 60 cm profile in the downslope boundary of the infiltration area (figure 5). The probes were set up into the regolith (TDR, 1, 3, 4, 7, 8, 9) and into marl blocks (TDR 2, 5, 6, 10, 11 and 12) with a stratification perpendicular to the vertical axe. Measurements were recorded every 20 minutes.

3.4. Surface runoff measurement

The very beginning of surface runoff was observed about 25 min after the start of the rainfall simulation. This overland flow used natural surface preferential pathways or handmade gullies according to the evolution of flow condition. Within 2 hours, only 3 gullies made it possible to concentrate total overland flow. Discharge measurements began 2.7 h after the

start of the experiment. Volumetric gauging was carried out every 60 min during the first 13 h and every 200 min over the remaining time.

Over the last 15 hours of the experiment, stream discharge was measured upstream and downstream the plot by volumetric gauging to assess the subsurface flow leaving the experimental plot. Downstream discharge value was assumed underestimated owing to unsuitable gauging conditions.

3.5. Sprinkling experiment

3.5.1. Rainfall

The experiment was carried out on the 9-12 of October 2009 over a period of 66.4 hours, interrupted with 2 to 58 minutes breaks to perform seismic refraction and LIDAR measurements, and to allow the generator and the pump to cool down. The actual duration of the rainfall simulation was 58 h. Rainfall intensity was constant over time but changed over area (fig. 6). The upper part of the plot was on average less irrigated than the lower part (3-4 mm.h⁻¹ against 11-12 mm.h⁻¹). The maximum intensity was 23 mm.h⁻¹ measured at the rain gauge 4 and the minimum intensity was 3 mm.h⁻¹ at the rain gauge 1. The mean rainfall intensity over the whole plot area was 10.2 mm.h⁻¹, which amounts to 68 m³ of injected water.

3.5.2 Artificial Tracing

Over the 35 first hours of the experiment (phase I), bromide (KBr) was used as tracer. From +35 h to the end of the simulation (phase II), bromide (KBr) together with chloride (KCl) were used as tracers. This procedure aimed at analysing the hydrological behaviour of the system over the gradual saturation of the soil. A total of 6 +/- 0.6 kg of bromide and 3 +/- 0.3 kg of chloride were injected.

Groundwater was sampled every 2 or 3 hours during the experiment. Event water (rainwater) sampling was more irregular. During the experiment, pH, redox potential, temperature and electrical conductivity were measured for each sample just after the sampling.

Bromide and Chloride as well as other major anions were analysed using ion chromatography techniques with a DIONEX DX 120 chromatograph. The relative uncertainty including measurement accuracy and repeatability error was lower than 3 %.

Due to imperfect mixing, Br⁻ and Cl⁻ concentrations in event water varied over time. Variations of Br⁻ input concentrations ranged from 54 mg.l⁻¹ to 137 mg.l⁻¹ and variations of Cl⁻ input concentrations ranged from 72 mg.l⁻¹ to 114 mg.l⁻¹. Input signal was then defined according to the incremental weighting technique proposed by (McDonnell et al., 1990) which consists in calculating the event water concentration weighting means from the rainfall fractions preceding the sampling time.

$$[T]_{EW,i} = \frac{\sum_{i=1}^n [T]_{EW,i-1} \times R_{i-1}}{\sum_{i=1}^n R_{i-1}}$$

where $[T]_{EW}$ is the event water concentration of tracer T (mg.l^{-1}); R is the actual duration of rainfall (h) (we consider rainfall intensity as constant during the experiment) and i is the incremental time step (h)

The incremental time i was 3 h according to the rainwater sampling time step.

Assuming that Br^- and Cl^- behave as conservative tracers, a mixing approach was used to estimate the origin of water in samples collected at various times and depths.

We note, EW_I , the event water contribution calculated from the Br^- variation over the phase I of the experiment, EW_{II} , the event water contribution calculated from the Cl^- variation over the phase II of the experiment and PE, the pre-event water.

Over phase I, a single tracer was injected and the set of mixing equations was:

$$EW_I(t) = \frac{[Br^-](t) - PE \times [Br^-]_{PE}}{[Br^-]_{EW_I}}$$

$$PE(t) = 1 - EW_I(t)$$

Where $\text{EW}_I(t)$ and $\text{PE}(t)$ are event water I ratio and pre-event water ratio respectively (-), $[Br^-]_{EW_I}$ and $[Br^-]_{PE}$ are the event water I and pre-event groundwater bromide concentration respectively (mg.l^{-1}) and $[Br^-](t)$ are the groundwater bromide concentrations according to time sampling (mg.l^{-1}).

A long term hydrochemistry monitoring (2004-2007) showed that bromide was not naturally present in groundwater, so that

$$EW_I(t) = \frac{[Br^-](t)}{[Br^-]_{EW_I}}$$

During the phase II, chloride was added as a second tracer. Mixing equations are then:

$$EW_{II}(t) = \frac{[Cl^-](t) - PE(t) \times [Cl^-]_{PE}}{[Cl^-]_{EW_{II}}}$$

$$PE(t) = 1 - EW(t) = 1 - \frac{[Br^-](t)}{[Br^-]_{EW}}$$

$$EW_I(t) = 1 - EW_{II}(t) - PE(t)$$

Where $EW_{II}(t)$ are event water II ratio (-), $EW(t)$ are the event water I+II ratio (-), $[Cl^-]_{EW_{II}}$ and $[Cl^-]_{PE}$ are the event water II and pre-event groundwater chloride concentrations respectively ($mg.l^{-1}$) and $[Cl^-](t)$ are the groundwater chloride concentrations according to time sampling ($mg.l^{-1}$).

Chloride concentration in event water I, $[Cl^-]_{EW_I}$, was 0 ($mg.l^{-1}$).

The mean initial concentration of chloride in the groundwater $[Cl^-]_{PE}$ was $1.7 mg.l^{-1}$ (STD : $1 mg.l^{-1}$; average value from 11 piezometers over $500 m^2$ area and a 2 years monitoring)

4. Results

4.1. Water balance and hydrological behaviour

Runoff coefficient increased with time according to a power function and reached 50 % at the end of the experiment (final flow rate was $5.2 mm.h^{-1}$, figure 7). The total runoff volume was $26 m^3$, that is to say 40 % of the sprinkling water amount. Actual evaporation was ignored, as it proved very low compared to the other terms of the water budget ($1 mm.day^{-1}$). As steady sprinkling rate was assumed, infiltration rate variation was symmetrical to that of surface runoff and decreased steadily according time. At the end of the experiment, the mean infiltration rate was $4.9 mm.h^{-1}$. Tracers mass balance confirmed the conservative behaviour of the tracers by showing that 40 % of bromide and 35 % of chloride were recovered in surface water.

The upstream discharge in the Laval torrent was around $8 l.min^{-1}$. Mean concentration in bromide was $4 +/- 0.5 mg.l^{-1}$. The downstream discharge was around $16 l.min^{-1}$. Average bromide concentration in the streamwater was $35 +/- 4 mg.l^{-1}$. The upstream-downstream variation both in terms of discharge and tracers showed the impact of the rainfall simulation on the stream regime. The difference could be attributed mainly to overland flow (estimate around $10 l.min^{-1}$).

The mean initial soil moisture along the 60 cm profile was 22.5 % (standard deviation: 3.8 %). Figure 8 shows the volumetric water content time series in marl blocks and weathered marl. The trend was similar for both weathering conditions of the marl although the dynamics were different. In both cases, the material moisture content rose sharply (5 % increase over the first 2 hours) and only increased slowly after around 10 mm of rainfall. Surface probes TDR 1, 3 and 4 were highly dependent on rainfall breaks and do not fit the general trend. Overall, the probes time response increased with depth. For example, the first soil moisture variation was observed after 3 mm of rainfall with shallow TDR 7 and after 10 mm with the deeper TDR 6. But exceptions are worth being mentioned. Changes in soil moisture were observed sooner with deep TDRs 11 and 12 (5 mm of rainfall) than with surface TDRs 3, 4 and 8 (8 mm of rainfall). In the regolith upper layer (roughly first meter depth), soil moisture distribution according to depth was shown to depend on preferential pathways set up by matrix/blocks interaction and blocks. As expected, soil water content was lower in the blocks (from 27 to 31 %) than in the regolith (33 to 36 %). The variations observed after this time were attributed to the rainfall breaks and the evaporation fluxes. TDR7 and TDR8 showed a special case where marl was saturated only 2 hours after the start of the rainfall. In this case, the probes were implemented below a depression in ground (see figure 5). During the saturation phase, no time lag was observed ($>$ time step = 20 min) owing to the great drainage capacity of the matrix. Once the rainfall was interrupted, water content dropped according to 2 recession curve shapes. A sharp decrease over the first 6 hours was attributed to the fast drainage of an active matrix porosity. This active porosity averaged 2 % in the blocks and 4 % in the regolith. The subsequent drainage mode was due to the emptying of a second, finer porosity.

No water was observed in the piezometers prior the experiment except in AE (upper part, 3.02 m deep) where water level was measured at 2.66 m depth. Groundwater variation was measured using recording devices in 6 piezometers (figure 9). All these piezometers were at least 2 m deep except BC (1.89 m). The hydraulic impact of the recharge was observed everywhere after 20 to 30 h of experiment. In most piezometers, the steady state was reached between + 25 h and + 35 h. The quickest reaction was observed in BC (5 h.) and the slowest in BD (30 h). As BC is deeper than BD (1.89 m versus 0.77 m), the water table dynamics shows that soil saturation started to rise in depth from rapid vertical flow and then increased upwards. The water level variation ranged from 0.15 m to more than 1 m (CH). The recession period started 1h15 after the end of rainfall. Water levels recovered their initial value in less than 5 hours for small variations ($<$ 25 cm) and between 6 and 20 hours for higher variations ($>$ 30 cm) except for CH.

At the hillslope scale, the results confirmed that water table was limited downwards by the marl bedrock. But the lateral continuity of this aquifer is broken by the marl blocks scattered over the landslide. Local perched water tables formed over the larger blocks (or block accumulation) and acted as transient water storage which contributes to the water flow redistribution both laterally and according to depth (total head in BD or BC was higher than in AC although more downstream)

4.2. Water tracing

4.2.1. Results

The tracing results are summarized in figure 10. Total event water contributions ranged between 21 % and 75 %. In 2/3 of the observation wells, EW contribution was lower than 50 %. The greatest contributions were observed in the shallowest boreholes. In detail, changes in EW contributions over time showed similarities between the observation wells although proportions varied:

- PE contributed predominantly at the very beginning of the experiment in piezometers where an initial water level was observed (AE). This is also the case in BC where water level measurements and water sampling could be carried out promptly after the start of rainfall.
- PE contribution dropped steadily until total rainfall amounted to about 200 mm. (AE, BC). In most piezometers, the first sampling could start only after 50 mm of rainfall at least, more than 100 mm in most cases. At this time, EW contribution was still rising. As already observed in AE and BC, 200 mm cumulative rainfall was needed to reach the minimum PE contribution (AC, DD, DB).
- From this threshold to a total of 450 to 550 mm of rainfall, PE contribution started to rise steeply before reaching a nearly constant value (AC, BC, DC, DD, DB). The trend was similar in AE but the rise of PE contribution was lower and shorter.
- The last part of the experiment was characterized by a new decrease of PE participation. According to the observation points, the drop of PE occurred mostly in favor of EW_I (CA, AC, DD, CE) or EW_{II} (AE, BC, CF, DB, DC). After the experiment, a 30 days hydrochemical monitoring was carried out in the piezometer AE. Most of the other wells dried out shortly after the end of the experiment. Pre-event water contribution rose rapidly from 28 % to 80 % in 58 h. The proportion was 97 % a week later (figure 11).

4.2.2. Uncertainties

The variation over time of input concentrations was a major drawback of the mixing approach carried out in this study. These changes have been taken into account by using the incremental weighting technique method (McDonnell et al., 1990, see section 3.5.2.). This technique aims at removing from the event water composition at time t all the rainfall fractions which have not yet fallen. At the end of the rainfall event, the event water concentration used in the mixing equations is the full event water weighted mean. This approach assumes that all the successive rainwater fractions are contributing to the flow but their impact is decreasing over time. Another calculation mode consists in using the discrete event water concentration. In this case, the rainfall fraction is assumed to be instantaneously available for contribution to total flow. These 2 procedures provide the extreme values of the components proportion. Minimum and maximum values were obtained from either of them depending on the time variation of the input signal (fig. 12). The participation of the flow components has been calculated using both of these techniques (fig. 10). The results showed that the differences between calculated proportions over the entire event according to the computing modes ranged from 6 % to 28 % for PE, 21 % to 32 % for EW_I , and 22 % to 25 % for EW_{II} . The impact of input concentration changes on the proportion estimates was different according to the relative importance of each component. The lowest ratios for PE were found in the deep piezometers AC and CA where PE participation proved to greatly dominate the flow (70 % and 79 % respectively).

Figure 10 shows that the variation of event water concentrations did not modify the general shape of the contributions time series. This result proves that the differences between the components labeling were significantly larger than the temporal changes. One of the main assumptions of water tracing was then respected. This important observation implies that the input uncertainties resulted in large errors in the contributions estimates but do not challenge the successive functioning steps described previously.

5. Discussion

5.1. Structure properties of marl and reservoirs interaction

Macroscopic observation of the material together with soil moisture and water table data made it possible to propose a hydrological concept involving several active reservoirs. (Figure 13). Active porosity of the soil matrix can be described using 2 main components: the structure porosity where drainage stops soon after the rainfall and the texture porosity where few days are needed to drain water.

The structure porosity is due to the flaked structure of marl. It is defined in the material part which has only undergone the primary stage of mechanical disaggregation of blocks. The material is quite coarse with up to several mm long flakes. At this stage, the oriented structure of the elements has been kept from the marl blocks. This structure porosity may also exist in the blocks (as shown in section 4.1.) according to their weathering level.

In a next stage of evolution, a mechanical and chemical weathering produces a silty to silty-clay sediment with a texture porosity. Over the weathering process, all the intermediate textures are expected until pure clay. Aside the active texture porosity, more clayey patches with high water content but poorly drainable may exchange with the active reservoirs. Diffusion processes are expected to supply/release part of infiltrated water in/from this microporosity. These processes involve longer time scales that prevent any contribution of the stored water at the event time scale. Even at longer time scales, this immobile water is supposed to play a minor role in the water budget as pure clay bodies were not widely represented in the field.

Blocks macroporosity was shown to provoke a rapid saturation in the subsoil. Unlike it is commonly observed in clayey material, the Draix black marl is not known to expand and shrink much according to whether the soil is dried out or wetted. This is first explained by the absence of smectite types clays in the material mineralogy. The chemical content of pore water is also known to change the behaviour of clay particles. Especially, the swelling capacity of clays (even smectites or interstratified as well as illite) increases greatly when the Na content of water is high (Yilmaz and Civelekoglu, 2009), which is not the case at Draix. Accordingly, there are no extended fissures or deep cracks which can drain water rapidly to the deeper layers. The reservoir involved is made of large voids formed by blocks layout and blocks decompression. The nature of macroporosity may be quite different in other clay shale environments. For example, large and deep cracks are usually observed at the Super-Sauze site (Debieche et al., 2011). The differences in soil structure and hydraulic properties can be

explained by the type of dominant clay minerals (interstratified at Draix against illite at Super-Sauze) and the Na content of pore water (very high at Super-Sauze).

5.2. Conceptualizing changes of infiltration over time and space at the hillslope scale

5.2.1. A perceptual model of groundwater recharge

A large variation in the hydraulic and hydrochemical behaviours according to the observation well was expected owing to the high soil heterogeneity and anisotropy described previously. Surprisingly, the contributions of the respective components varied in a quite reproducible way over time and area and a general behaviour concept may be proposed. Of course, local heterogeneities made that the relative values of the components participation as well as the timing of the processes changed according to the observation boreholes. For purposes of parsimony, a perceptual model is proposed with 3 reservoirs according to the 3 main active porosities encountered in the medium. These 3 reservoirs can be distinguished each other by their respective water retention capacity depending on the pores size and the clay content. In the soil volumes where the major part of voids is made of blocks macroporosity, water retention strengths are expected lower than gravity. Conversely, the proportion of water retained on the grains or within the micropores should increase as texture porosity dominates the pores volume. The structure porosity of flakes represents an in-between situation. Water pressure needed to produce water flow increases as retention capacity is getting stronger. In a conceptual point of view, this situation may be represented as pressure head thresholds in the reservoirs. At the end of the experiment, the mean infiltration rate was in the lower part of the field hydraulic conductivities range. This shows that a larger scale approach resulted in a decrease of the soil water transfer capacity. This result emphasizes the importance of micropores volume in the total porosity as area increases. This is in keeping with other experimental approaches showing that macropores were only a small part of total porosity (German and Beven, 1981). The proportion of active porosity proved to range between 1 % and 5 % according to the soil type, the nature of the macropores and the experimental devices (Bouma and Dekker, 1978; Germann and Beven, 1981; Boolting et al., 1993; Di Pietro et al., 2003)

Accordingly, blocks macroporosity was assumed lower than structure porosity, and structure porosity was supposed lower than texture porosity. Figure 14 shows the possible steps of the recharge mechanism:

Initial step: Before the rainfall starts, water level in the different reservoirs of the unsaturated zone was lower than the flow thresholds.

Step 1: As rainfall began, water used preferential pathways and event water contributed to the groundwater recharge, Event water contribution rose steadily over the first 200 mm of gross rainfall, namely a total of about 80 mm of net rainfall (infiltration). This amount was partly used to renew water in the blocks macroporosity and, for another part, it should feed the structure porosity. According to local situations (relative size of the reservoirs), total porosity

was mainly made of blocks porosity which resulted in a large contribution of EW (BC, DE) or structure porosity, so that the proportion of EW did not exceed 50 % (mainly deep piezometers, CA, AC, AE). This is in keeping with the quicker hydraulic reaction observed in piezometer BC than in piezometer AC

Step 2: Water table reached a nearly constant level after around 80 mm of net rainfall. The structure porosity was saturated but was mainly filled by pre-event water. The reservoir contributed to the flow, partly via the blocks macropores and also supplied water to the texture porosity. The latter was saturating slowly and ended up exchanging with related reservoirs. Thus, PE contribution was assumed to rise up by the successive activation of structure and texture porosities. In most piezometers (AC, DD, AE, BC, CF, DB), PE contribution reached a sort of stage ranging from 50 to 80 % until cumulative rainfall was 450 to 550 mm (around 180 mm to 220 mm of net rainfall). This situation illustrated a balance between the dominant contribution of event water from the blocks porosity and that of pre event water from structure and texture porosities.

Step 3: After 180 mm to 220 mm of net rainfall (depending on the observation borehole), water in the structure porosity was fully renewed and event water contribution rose up again. The use of a second tracer from $t=35$ h showed that the variation of EW_{II} contribution was similar to that of EW_I at the beginning of the experiment. This confirmed the still important role of the blocks porosity on the event water transfer. At the end of the experiment, pre-event contribution ranged from 10-20 % (in the shortest piezometers, DB, DC) to 60 % in some of the deepest piezometers (CA, AC).

A last step occurred as soon as rainfall stopped. The drainage differential between the reservoirs resulted in an inversion of the hydraulic gradients and a major contribution to total flow of the structure porosity. This participation may arise partly via the blocks porosity. The same situation occurred between the texture porosity (mainly pre-event water) and the structure porosity. The result was a rapid rise of the pre-event contribution showed by the return to the initial tracer concentration (figure 11).

This 3 components model proposes modes of interactions between the different active porosities. The concept helps explaining the pre-event water contribution to the groundwater recharge. This pre-event participation during the experiment emphasizes the topical questions about the “old water paradox” (Kirchner, 2003). In the proposed concept, the soil saturation rate is a key point explaining the remobilization of pre-event water. Kienzler and Naef (2008) also observed this relation in situ and showed the important role of interactions between micropores and macropores reservoirs.

The specificity of the studied material is the high contrast of the drainage and storage capacities according to the weathering rate. This contrast is mostly due to the clayey nature of the marl which favors preferential pathways (blocks/regolith contact or shrinkage cracks) and produces a range of matrix porosities (from a high drainage flake-induced porosity to a poorly transmissive clayey microporosity). These properties are common to similar clayey materials and the proposed conceptual model should be applied to other marl regolith or shale. However, the relative contributions of these porosities will change according to the type of clay and the pore water chemistry. The proportion of shrinking clays and the Na content in

pore water will control the formation and geometry of cracks, and the type of clays together with the carbonate-clay ratio will have an impact on the microstructure of the material (nature of the flakes)

5.2.2. Processes involved in the pre-event water participation

The change in pre-event water contribution during rainfall is an original mechanism which is not much described. The high celerity of the pre-event water restitution implies an efficient transfer process. As proposed by McDonnell (1990) and discussed recently in Kienzler and Naef (2008), one solution could be the release of pre-event water in larger pores from saturated patches in the soil matrix. Potential gradient should be invoked to get water out of the microporosity, but it is unlikely to occur as macropores should be saturated too. The piston flow mechanism (Hewlett and Hibbert, 1967) could also be considered but it is usually not suitable to explain flow processes in soils. Indeed, the capacity of new water to « push out » older water requires a tube-liked system in which the soil layer is confined between two impervious boundaries. Moreover, the pores volume of the active soil layers should be very small compared with the input flux. These situations are seldom observed in natural soils. Nevertheless, such a mechanism could arise in our case owing to the peculiar structure of the material. The weathered regolith cut up according to oriented layers of flakes can lay out longitudinal voids limited by impervious boundaries. At the microscale, the displacement of successive nearly undisturbed water layers is likely to occur. At the macroscale, a certain degree of mixing is expected between water layers resulting in a dispersion effect but this assumes that there is a continuity of the layering nature of soil across scales. At last, Williams et al (2002) proposed another translatory flow process based on a transient state kinematic wave effect. This mechanism was mainly described on soil columns at the laboratory scale (Rasmussen et al., 2000). It is supposed to transmit water by a rising up of the local hydraulic gradient which caused redistribution of water. Pressure responses are deemed to have celerity 500 times faster than actual water velocity (Williams et al., 2002). However, these mechanisms are not fully understood (Mc Glynn et al, 2002) and their efficiency (even their existence) at the hillslope scale has still to be clarified.

5.2.3. Material structure and pores connectivity

Even if the physical mechanism of water transfer was not fully understood, the results showed that the efficiency and timing of the pre-event water release were reproducible over area. Our extensive rainfall simulation showed that the results were not area-dependent and were depth-dependent only to a small extent. It was not possible to relate significantly the local hydrological behavior to surface features (local topography, slope, blocks outcropping) or to subsurface properties (position, areal extent of marl blocks, subsurface topography). This proves that the processes involved are more dependent on the intrinsic material structure than on the hillslope scale soil heterogeneity. This can be explained by the close relation between connectivity and structure. The notion of connectivity is usually defined for fractured medium as the “density of fractures that intersect sufficiently to promote flow” (de Marsily, 1985). In porous medium, definition of connectivity requires basic topological properties such as the number of isolated pores, the number of redundant connections within the pores space and the number of closed cavities (Vogel, 2002). These properties are not randomly distributed and

soil formation processes usually result in continuous structures that control water flow (Weiler and Naef, 2003b; Kienzler and Naef, 2008; Schaap et al., 2008). The longer are the disconnected preferential flow paths, the larger is the proportion of flow in the structure porosity. This results in a large contribution of pre-event water. Conversely, when preferential flow paths are correctly connected, water infiltrates readily in the deep layers of the soil without exchanging much with pore water, so that pre-event water contribution decreases. The degree of connectivity of water pathways should be considered as a first order property to explain the hydrological consequences of heterogeneity. It is also regarded as a convenient descriptor of small scale behavior helping parameterization of the effects of heterogeneity across all scales (McDonnell et al., 2007). The connectivity as an integrative property of the soil structure is most certainly a key point in the hydrological behaviors observed in the well-structured material of this study.

5.3. Upscaling at the hillslope and catchment scales

As shown in section 4.1., no subsurface flow was detected in the stream downwards during the experiment. At the end of the experiment, the stream discharge variation upstream and downstream the landslide was 8 l.min^{-1} while rainfall rate was 17 l.min^{-1} . At that time, steady state conditions were not fully obtained yet. Owing to the large depth and high hydraulic conductivity of the regolith together with the low initial soil moisture content, part of subsurface water could have been used to saturate the surrounding material.

The question of the marl bedrock as a true zero-flux boundary can also be addressed. In this region, the “Terres Noires” formation has been successively fold-thrusted (Digne Nappe settlement) after the Oligocene which resulted in all-scales fractures networks. From borehole image analysis, Lofi et al. (2011) confirmed that partly-opened fissures could be observed in the bedrock. Tracer tests and hydrogeological monitoring showed that these fissures could act as preferential pathways for water flow and that flow direction was strongly constrained by structural and sedimentological discontinuities (Garel, 2010). Neuville et al. (2011) have obtained scaling laws of the aperture and thickness of discontinuities in the Draix black marl using techniques for the aperture reconstruction of fissures. They used these geometrical properties to get the macroscopic hydraulic transport properties of discontinuities and concluded that fractured marl was potentially highly permeable. Finally, Cras et al., 2007 showed from an environmental tracing investigation at the catchment scale that deep water from the marl bedrock could contribute to the low flows. With a different dataset, Garel (2010) provided similar conclusions using the same technique. These processes were observed elsewhere. De Montety et al. (2007) showed that a deep recharge from preferential fractures pathways was likely to occur at the Super-Sauze landslide. All these independent results indicate that preferential pathways are present in the fractured marl bedrock. They can drain or recharge the shallow saturated zone according to the current hydraulic conditions of the regional and local hydrogeological systems. At Draix, there is a significant probability that infiltrated water during the experiment was partly lost in the substratum via open fractures.

5.4. Landslide initiation

In civil engineering, slope stability analysis is usually carried out assuming homogeneous soil properties although it is widely accepted that hillslope instability is mainly triggered by preferential flow producing sharp changes in pore water pressure (Vieira et Fernandes, 2004). In recent years, spatial variability of soil features has progressively gained importance in soil mechanism calculation and slope stability numerical modelling. For example, Srivastava et al. (2010) showed that an increase of the hydraulic conductivity variability resulted in a decrease of the factor of safety. This illustrates the beneficial role of active porosity in the water drainage away of the zone at risk. The situation may however be quite different in the case where the type of porosity changes over area. This is typically the situation encountered in soils where the water flow continuity in the matrix is disturbed by channel flow through natural pipes or fractures/cracks network. Some authors identified that the presence of soil pipes networks had adverse effects on landsliding (Jones, 1997; Zhu, 1997). Pipes can carry water at greater depth than would be possible by darcyan-type infiltration. As Hencher (2010) stated, these pipes may be formed in a situation of early landslide movements and may seasonally be clogged or collapse resulting in closed-end pipes and excessive water pressure. If the soil structure does not change over time, channel flow can also be regarded as a way to enhance drainage and reduce water pressure as we would do using an artificial horizontal drain system. In our study, water could be carried deeply through macropores formed at the interface between marl blocks and regolith. In most cases, an efficient drainage was observed after the rainfall. The terrain morphology provides one explanation of this behaviour. The infiltration area was situated downslope in the accumulation zone where the slope of the substratum drops dramatically (fig 1). In spite of the exceptional amount of input water (nearly 680 mm of rainfall in few days), LIDAR measurements showed that the landslide was not reactivated over the rainfall simulation (Travelletti et al, 2011). A 2 years GPS monitoring showed that no significant changes affected the landslide morphology although piezometers were displaced according to a pure translatory movement (Garel, 2010). The landslide is moving slowly according to a mass displacement and no acceleration was observed owing to the concavity of the bedrock topography. In this context, the nature of macropores may change by silting up or collapse due to the progressive on spot chemical and mechanical weathering of the material. In an early stage, the large drainage capacity of soil is expected to relieve water pressure. The subsequent clogging effect of the larger pores occurs slowly so that large scale isolated dead-end macropores are quite unlikely. In such context, an hillslope scale mass bursting hazard is limited. Even though the material is very similar, the situation proves different at Super Sauze (Debieche et al., 2011) where the landslide intense activity is due to steeper slope conditions and fast deep transversal transfer of water according to the fissures network. In this context, part of the fissures network happens to be isolated and no more connected to the drainage system. In these situations, tracers confirmed that deep groundwater level variations were explained by pressure transfer. Such processes may dramatically increase pore water pressure and result in local slope instabilities.

Multi-scale interdisciplinary studies at Draix (Cras et al., 2007 ; Lofi et al, 2011 ; Neuville et al., 2011) showed that the marl substratum comprised open fractures where water could flow preferentially. As Lofi et al. (2011) stated, these preferential pathways have possible important consequences for landslide generation. The high anisotropy of the marl favors

ruptures along the schistosity and fracture planes. Chemical weathering induced by preferential water circulation is also suspected to create weakness zones from new or preexistent discontinuities. These deep discontinuities may result in slope rupture and hydrological-triggered landslides when combined with other factors (slope gradient, seismic activity).

These results show that a simplified analysis based on the average nature of material is not convenient. A prior combined investigation of the geomorphological, hydrological as well as hydrochemical context is required to improve our ability to forecast landslide processes.

Conclusion

A large scale simulated rainfall enabled us to clarify several aspects of infiltration conditions in unstable marl hillslopes. Results from soil moisture and water table monitoring together with water tracing gave insight into the infiltration modes over time and space in a well-structured soil context. Active reservoir interactions proved very dependent on the material structure, emphasizing the major role of macropores connectivity.

Despite the large heterogeneity and anisotropy of the medium, few reproducible functional traits could be deduced from this experiment. A perceptual model was proposed to explain the variation of pre-event water contribution over time. This was achieved using a concept based on 3 structure-driven porosities. Although simplified, this 3 reservoirs vision of the hillslope was deduced from careful in situ observations of the material structure combined with information from multi-scale hydrodynamic data. This approach is in keeping with the topical idea that the detailed study of process complexity should result in extracting the most relevant field descriptors of the flow processes. This approach is expected to allow watershed classification and scale transfer. At least 2 future issues should be addressed to deal with this challenge. Although widely observed in all possible contexts, the release of pre-event water from the poorly functional microporosity to the active porosity is generated from physical mechanisms which are still unknown. We argue that the soil structure from which pores number, pores size, pores shape, and the integrative notion of connectivity should be deduced is one of the main soil driving properties of the pre-event water release processes. Accordingly, the second issue regards the way how this soil structure will be properly investigated on site. Nowadays more and more innovative techniques are available to study the soil structure, including 3D imaging. Unfortunately, they are still to be used in small samples in laboratory conditions. Bridging the gap between investigation scales would need to develop in situ shallow geophysics for soil structure imaging.

Acknowledgments

This work was carried out under the ECOU-PREF 'Écoulement préférentiels dans les versants marneux' research program (05-ECCO-007-04), funded by the French National Research Agency. The Draix ERBs has received the ORE label (Observatory for environmental research) from the French department of Research.

The Ph-D grant of E.Garel was supported by the Regional Council of Provence-Alpes-Côtes d'Azur.

The authors would like to thank, Nicolle Mathys (Cemagref), Olivier Maquaire & Mathieu Fressard (University of Caen-Basse-Normandie), Dominika Krezminska (Technical University Delft), Jean-Philippe Malet and Julien Travelletti (University of Strasbourg) and Gilles Grandjean (BRGM Orléans) for their support during the field experiment.

References

- Antoine, P., Giraud A., Meunier M., Van Asch Th. W. J., 1995. Geological and geotechnical properties of the "Terres Noires" in southeastern France: Weathering, erosion, solid transport and instability. *Engineering Geology* 40 (3-4): 223-234. doi:10.1016/0013-7952(95)00053-4.
- Boast, C.W. and Robertson, R.W., 1982. A micro-lysimeter method for determining evaporation from bare soil: Description and laboratory evaluation. *Soil Science Society of America Journal*, 46: 689-696.
- Booltink, H.W.G., Hatano, R., Bouma, J., 1993. Measurement and simulation of bypass flow in a structured clay soil: a physico-morphological approach. *Journal of Hydrology*, 148, 149-168
- Bouma, J. and Dekker, L. W., 1978. A case study on infiltration into dry clay soil. I Morphological observations. *Geoderma*, 20, 27-40
- Bryan R. B., and Jones J.A.A., 1997. The significance of soil piping processes: inventory and prospect. *Geomorphology* 20(3-4): 209-218. doi:10.1016/S0169-555X(97)00024-X.
- Canton Y., Sole-Benet A., Domingo F., 2004. Temporal and spatial patterns of soil moisture in semiarid badlands of SE Spain. *Journal of Hydrology* 285(1-4): 199-214. doi:10.1016/j.jhydrol.2003.08.018.
- Cantón, Y., Domingo F., Solé-Benet A., et Puigdefábregas J., 2001. Hydrological and erosion response of a badlands system in semiarid SE Spain. *Journal of Hydrology* 252(1-4): 65-84. doi:10.1016/S0022-1694(01)00450-4.
- Cras A, Marc V., Travi Y., 2007. Hydrological behaviour of sub-Mediterranean alpine headwater streams in a badlands environment. *Journal of Hydrology* 339(3-4): 130-144. doi:10.1016/j.jhydrol.2007.03.004.
- Debieche T.H., Bogaard T.A., Marc, V., Emblanch C., Krzeminska D., Malet J.-P., (XXXX). Hydrological and hydrochemical processes during a large-scale infiltration experiment : Super Sauze mudslide (France). *Hydrological Processes*, in press, DOI: 10.1002/hyp.7843
- Descroix L., Mathys N., 2003. Processes, spatio-temporal factors and measurements of current erosion in the French Southern Alps: A review. *Earth Surface Processes and Landforms* 28(9): 993-1011. doi:10.1002/esp.514.
- de Marsily, 1985. Flow and transport in fracture rock. Memoires. Hydrogeology of rocks of low permeability. Intern. Assoc. Hydrogeol., Tucson, Ariz. 267-277.

Di Pietro, L., Ruy, S. and Capowiez, Y. 2003. Predicting preferential water flow in soils by traveling-dispersive waves. *Journal of Hydrology*, 278, 64-75.

Esteves, M., Descroix L., Mathys N., Lapetite J.-M., 2005. Soil hydraulic properties in a marly gully catchment (Draix, France). *Catena* 63(2-3): 282-298. doi:10.1016/j.catena.2005.06.006.

Fressard, M., 2008. Le glissement de terrain du Laval Morphologie-Evolution-Cartographie (Draix, Alpes de Haute Provence, France). Master Thesis. Université de Caen Basse-Normandie.

Gallart F., Latron J., Llorens P., Rabada D., 1997. Hydrological functioning of mediterranean mountain basins in Vallcebre, Catalonia: Some challenges for hydrological modelling. *Hydrological Processes* 11(9): 1263-1272. doi:10.1002/(SICI)1099-1085(199707)11:9<1263::AID-HYP556>3.0.CO;2-W.

Garel, E., 2010. Etude des processus de recharge des nappes superficielles et profondes dans les versants marneux fortement hétérogènes. Cas des Terres noires des Alpes du sud de la France – ORE Draix. Ph. D. Dissertation, 180 p., Université d'Avignon et des pays de Vaucluse, France, nov. 2010.

Germann, P. and Beven, K 1981. Water flow in soil macropores. I an experimental approach. *Journal of Soil science*, 32, 1-13

Grandjean G., Hibert C., Mathieu F., Garel E., Malet J.-P., 2009. Monitoring water flow in a clay-shale hillslope from geophysical data fusion based on a fuzzy logic approach. *Comptes Rendus Geosciences* 341(10-11): 937-948. doi:10.1016/j.crte.2009.08.003.

Griffiths J.S., Hart, Mather A.E., Stokes M., 2005. Assessment of some spatial and temporal issues in landslide initiation within the Rio Aguas Catchment, South-East Spain. *Landslides* 2(3): 183-192. doi:10.1007/s10346-005-0004-1.

Hencher, S.R., 2010. Preferential flow paths through soil and rock and their association with landslides. *Hydrological Processes*, 24: 1610-1630. doi: 10.1002/hyp.7721

Hewlett, J.D. and Hibbert, A.R., 1967. Factors affecting the response of small watersheds to precipitation in humid areas. In International symposium in forest hydrology, Sopper WE, Lull HW (Eds). Pergamon: Oxford, 275-290.

Jones J.A.A., 1997. Pipeflow contributing areas and runoff response. *Hydrological Processes* 11(1): 35-41. doi:10.1002/(SICI)1099-1085(199701)11:1<35::AID-HYP401>3.0.CO;2-B.

Kienzler P.M., Naef F., 2008. Subsurface storm flow formation at different hillslopes and implications for the 'old water paradox'. *Hydrological Processes* 22(1): 104-116. doi:10.1002/hyp.6687.

Kirchner J.W., 2003. A double paradox in catchment hydrology and geochemistry. *Hydrological Processes*, 17: 871-874. doi: 10.1002/hyp.5108

Latron J., Gallart F., 2008. Runoff generation processes in a small Mediterranean research catchment (Vallcebre, Eastern Pyrenees). *Journal of Hydrology* 358(3-4): 206-220. doi:10.1016/j.jhydrol.2008.06.014.

Li X.Y., Gonzalez A., Sole-Benet A., 2005. Laboratory methods for the estimation of infiltration rate of soil crusts in the Tabernas Desert badlands. *Catena* 60(3): 255-266. doi:10.1016/j.catena.2004.12.004.

Lofi J., Pezard P., Loggia D., Garel E., Gautier S., Merry C., Bondabou K., (Accepted) Petrophysical, borehole geophysics and geological characterization of tectonized clay shales drilled at Draix (southern French Alps). *Hydrological Processes*, in press, DOI: 10.1002/hyp.7997

Lorente A., Garcia-Ruiz J.M., Beguena S., Arnaez J., 2002. Factors explaining the spatial distribution of hillslope debris flows - A case study in the Flysch Sector of the Central Spanish Pyrenees. *Mountain Research and Development* 22(1): 32-39.

Lukey B.T., Sheffield J., Bathurst J.C., Hiley R.A., Mathys N., 2000. Test of the SHETRAN technology for modelling the impact of reforestation on badlands runoff and sediment yield at Draix, France. *Journal of Hydrology* 235(1-2): 44-62.

Malet J.-P. (2003) Les glissements de type écoulement dans les marnes noires des Alpes du Sud. Morphologie, fonctionnement et modélisation hydro-mécanique. Thèse de doctorat. <http://eprints-scd-ulp.u-strasbg.fr:8080/26/>.

Maneta M., Schnabel S., Jetten V., 2008. Continuous spatially distributed simulation of surface and subsurface hydrological processes in a small semiarid catchment. *Hydrological Processes* 22(13): 2196-2214. doi:10.1002/hyp.6817.

Mathys, N., Brochot S., Meunier M., Richard D., 2003. Erosion quantification in the small marly experimental catchments of Draix (Alpes de Haute Provence, France). Calibration of the ETC rainfall-runoff-erosion model. *Catena* 50(2-4): 527-548. doi:10.1016/S0341-8162(02)00122-4.

Mathys, N., Klotz S., Esteves M., Descroix L., Lapetite J.-M., 2005. Runoff and erosion in the Black Marls of the French Alps: Observations and measurements at the plot scale. *Catena* 63, (2-3): 261-281. doi:10.1016/j.catena.2005.06.010.

McDonnell, J.J., Bonell, M., Stewart, M.K., Pearce, J. 1990. Deuterium variations in storm rainfall : implications for stream hydrograph separation. *Wat. Res. Research*, 26: 455-458.

McDonnell, J.J., 1990. A rationale for old water discharge through macropores in a steep humid catchment. *Wat. Res. Research.*, 26: 2821-2832.

McDonnell J.J., Sivapalan M., Vaché K., Dunn S., Grant G., Haggerty R., Hinz C. Hooper R., Kirchner J., Roderick M.L., Selker J., Weiler M., 2007. Moving beyond heterogeneity and process complexity: A new vision for watershed hydrology. *Water Resources Research* 43(7): doi:10.1029/2006WR005467

McGlynn BL, McDonnell JJ, Brammer DD, 2002. A review of the evolving perceptual model of hillslope flowpaths at the Maimai catchments, New Zealand. *Journal of Hydrology*, 257:1-26.

De Montety V. de, Marc V., Emblanch C., Malet J.-P., Bertrand C., Maquaire O., Bogaard T.A., 2007. Identifying the origin of groundwater and flow processes in complex landslides affecting black marls: insights from a hydrochemical survey. *Earth Surface Processes and Landforms* 32(1): 32-48. doi:10.1002/esp.1370.

Nadal-Romero E., Regues D., 2009. Detachment and infiltration variations as consequence of regolith development in a Pyrenean badland system. *Earth Surface Processes and Landforms* 34(6) 824-838. doi:10.1002/esp.1772.

Nadal-Romero E, Regues D., Latron J., 2008. Relationships among rainfall, runoff, and suspended sediment in a small catchment with badlands. *Catena* 74 (2): 127-136. doi:10.1016/j.catena.2008.03.014.

Neuville, A., Toussaint, R., Schmittbuhl, J., Koehn, D., Schwartz, J.O., 2011. Characterization of major discontinuities from borehole cores of the black consolidated marl formation of Draix (French Alps). *Hydrological Processes*, in press, DOI: 10.1002/hyp.7984

Rasmussen TC, Baldwin RH, Dowd JF, Williams AG, 2000. Tracer vs. pressure wave velocities through unsaturated saprolite. *Soil Science Society of America Journal*, 64: 75-85.

Regues D, Gallart F., 2004. Seasonal patterns of runoff and erosion responses to simulated rainfall in a badland area in Mediterranean mountain conditions (Vallcebre, southeastern Pyrenees). *Earth Surface Processes and Landforms* 29(6): 755-767. doi:10.1002/esq.1067.

Richard D., Mathys N. 1999. Historique, contexte technique et scientifique des BVRE de Draix. Caractéristiques, données disponibles et principaux résultats acquis au cours de dix ans de suivi. Actes du colloque "Les bassins versants expérimentaux de Draix, laboratoire d'étude de l'érosion en montagne", Draix, Le Brusquet, Digne, 22-24 Octobre 1997. CEMAGREF, Grenoble, 11-28.

Schaap JD, Lehmann P, Kaestner A, Vontobel P, Hassanein R, Frei G, de Rooij GH, Lehmann E, Fluhler H., 2008. Measuring the effect of structural connectivity on the water dynamics in heterogeneous porous media using speedy neutron tomography. *Advances in water resources*, 31: 1233-1241. doi: 10.1016/j.advwatres.2008.04.014

Srivastava A, Babu GLS, Haldar S, 2010. Influence of spatial variability of permeability property on steady state seepage flow and slope stability analysis. *Engineering Geology*, 110: 93-101. doi: 10.1016/j.enggeo.2009.11.006

Torri D., Colica A., Rockwell D., 1994. Preliminary study of the erosion mechanisms in a Biancana Badland (Tuscany, Italy). *Catena* 23(3-4): 281-294.

Torri D., Regues D., Pellegrini S., Bazzoffi P., 1999. Within-storm soil surface dynamics and erosive effects of rainstorms. *Catena* 38:131-150

Travelletti J., Malet J.-P., Sailhac P., Grandjean G., Ponton J., (2011). Monitoring of water infiltration in weathered clay shale slopes with Time-Lapse Electrical Resistivity Tomography. *Hydrological Processes*, in press, DOI: 10.1002/hyp.7983

Vieira B.C., Fernandes N.F., 2004. Landslides in Rio de Janeiro: The role played by variations in soil hydraulic conductivity. *Hydrological Processes* 18(4): 791-805. doi:10.1002/hyp.1363.

Vogel, H.J., 2002. Topological characterisation of porous media. In: Mecke, K., Stoyan, D. Ed. Morphology of condensed matter. Lecture notes in Physics, vol. 600. New York: Springer, 2002, p. 75-92.

Weiler M., Naef F., 2003b. An experimental tracer study of the role of macropores in infiltration in grassland soils. *Hydrological Processes* 17(2): 477-493. doi:10.1002/hyp.1136.

Wijdenes D.J.O., Ergenzinger P., 1998. Erosion and sediment transport on steep marly hillslopes, Draix, Haute-Provence, France: an experimental field study. *Catena* 33 (3-4): 179-200.

Williams AG, Dowd JF, Meyles EW, 2002. A new interpretation of kinematic stormflow generation. *Hydrological Processes*, 16: 2791-2803. doi: 10.1002/hyp.1071

Yilmaz I., Civelekoglu B., 2009. Gypsum: An additive for stabilization of swelling clay soils. *Applied Clay Science* 44(1-2): 166-172. doi:10.1016/j.clay.2009.01.020.

Zhu, T. X. 1997. Deep-seated, complex tunnel systems -- a hydrological study in a semi-arid catchment, Loess Plateau, China. *Geomorphology* 20(3-4): 255-267. doi:10.1016/S0169-555X(97)00027-5.

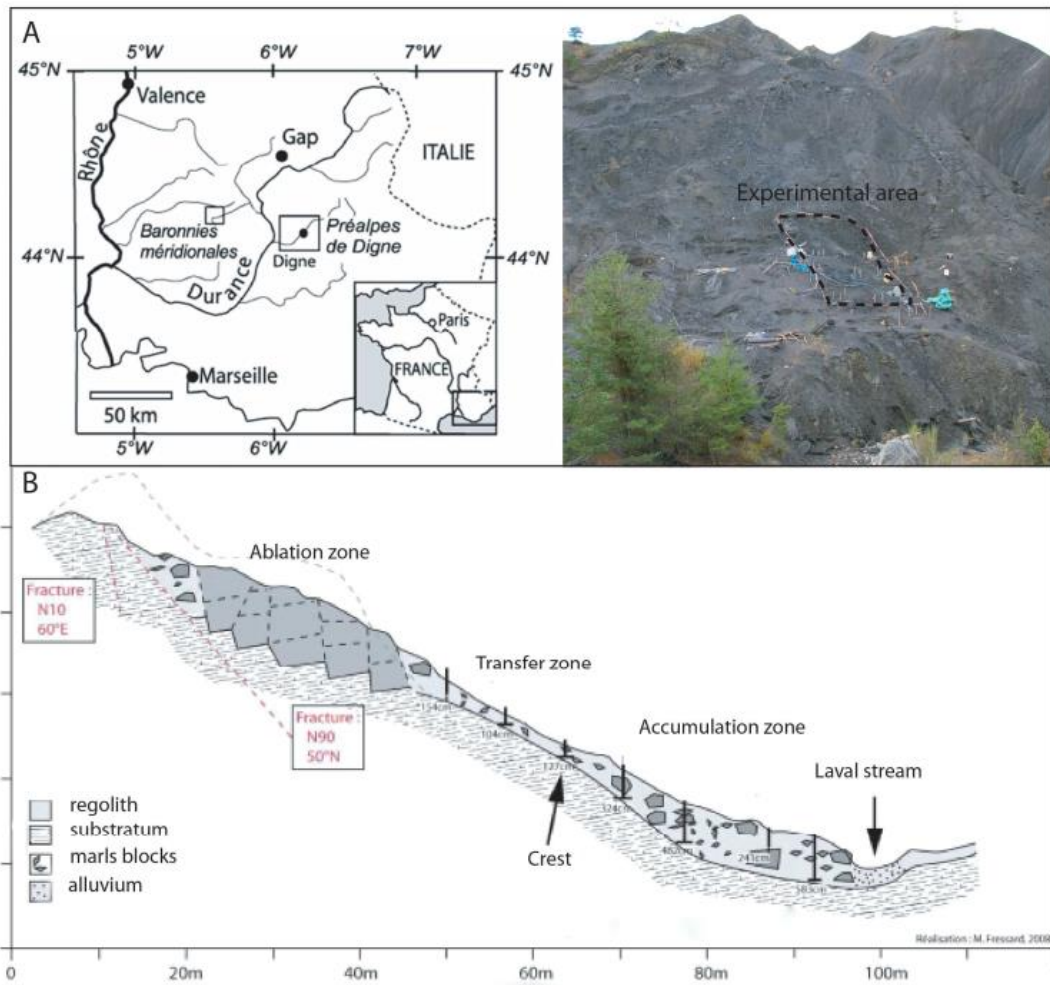
Tables

Line (aa')	Depth (m)	Line (bb')	Depth(m)	Line (cc')	Depth(m)	Line (dd')	Depth(m)
AA	1.86	BA	1.61	<u>CA</u>	<u>2.28</u>	DA	0.95
AB	0.87	BB	0.85	CB	0.94	<u>DB</u>	<u>1.54</u>
<u>AC</u>	<u>3.87</u>	<u>BC</u>	<u>1.89</u>	CC	1.30	<u>DC</u>	<u>1.03</u>
AD	0.57	<i>BD</i>	<i>0.77</i>	CD	0.88	<u>DD</u>	<u>1.71</u>
<u>AE</u>	<u>3.02</u>	BE	3.00	<u>CE</u>	<u>1.95</u>	DE	0.97
AF	1.45	BF	0.94	<u>CF</u>	<u>1.97</u>	DF	1.00
AG	1.00	BG	2.42	CG	1.00		
				<i>CH</i>	<i>3.40</i>		

Table 1 : Piezometers depth according to their line position. Wells name underlined are those where water could be sampled. In italic are those where water was not sampled but level could be measured.

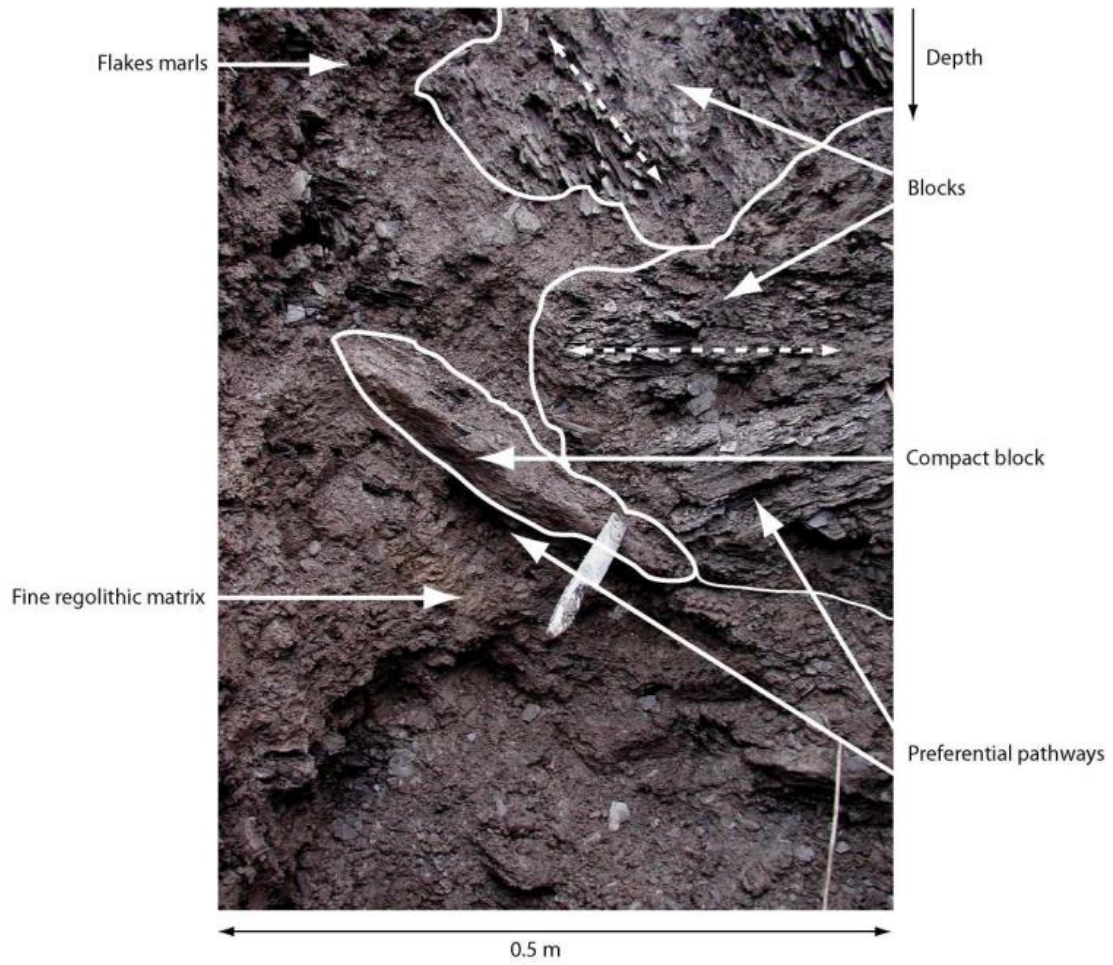
FIGURES

FIGURE 1 :



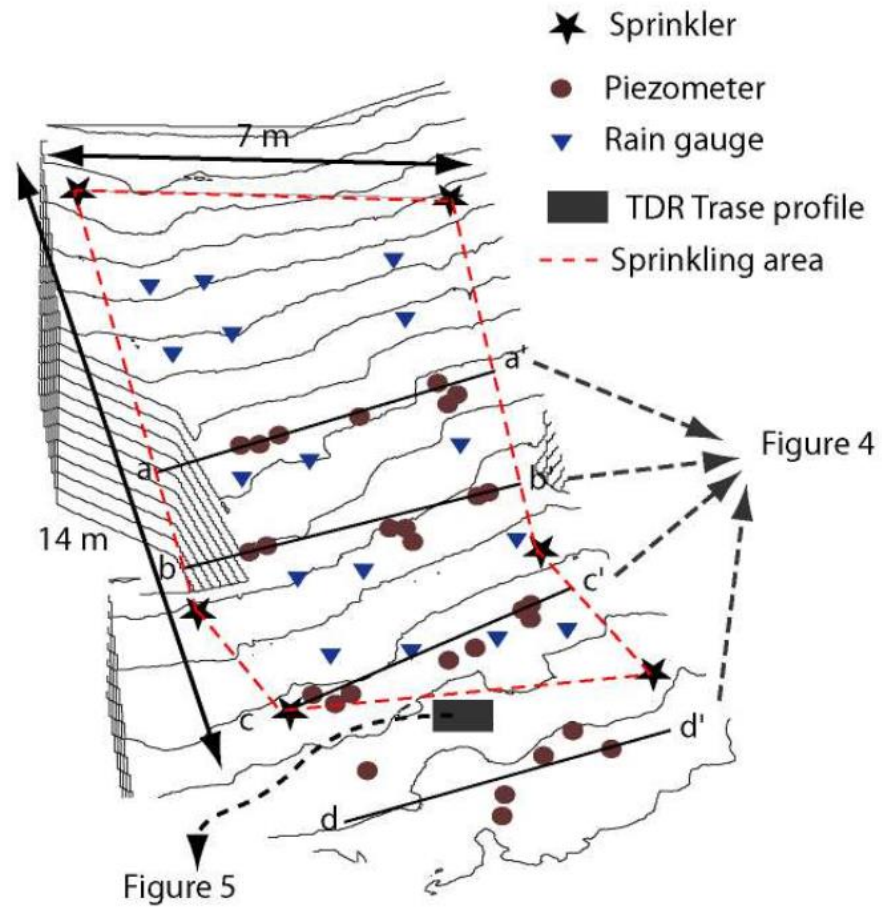
Location of the Draix ERB's (From Descroix and Mathys, 2003) and view of the landslide and the experimental plot. B. Cross section of the landslide (from Freyssard, 2008)

FIGURE 2 :



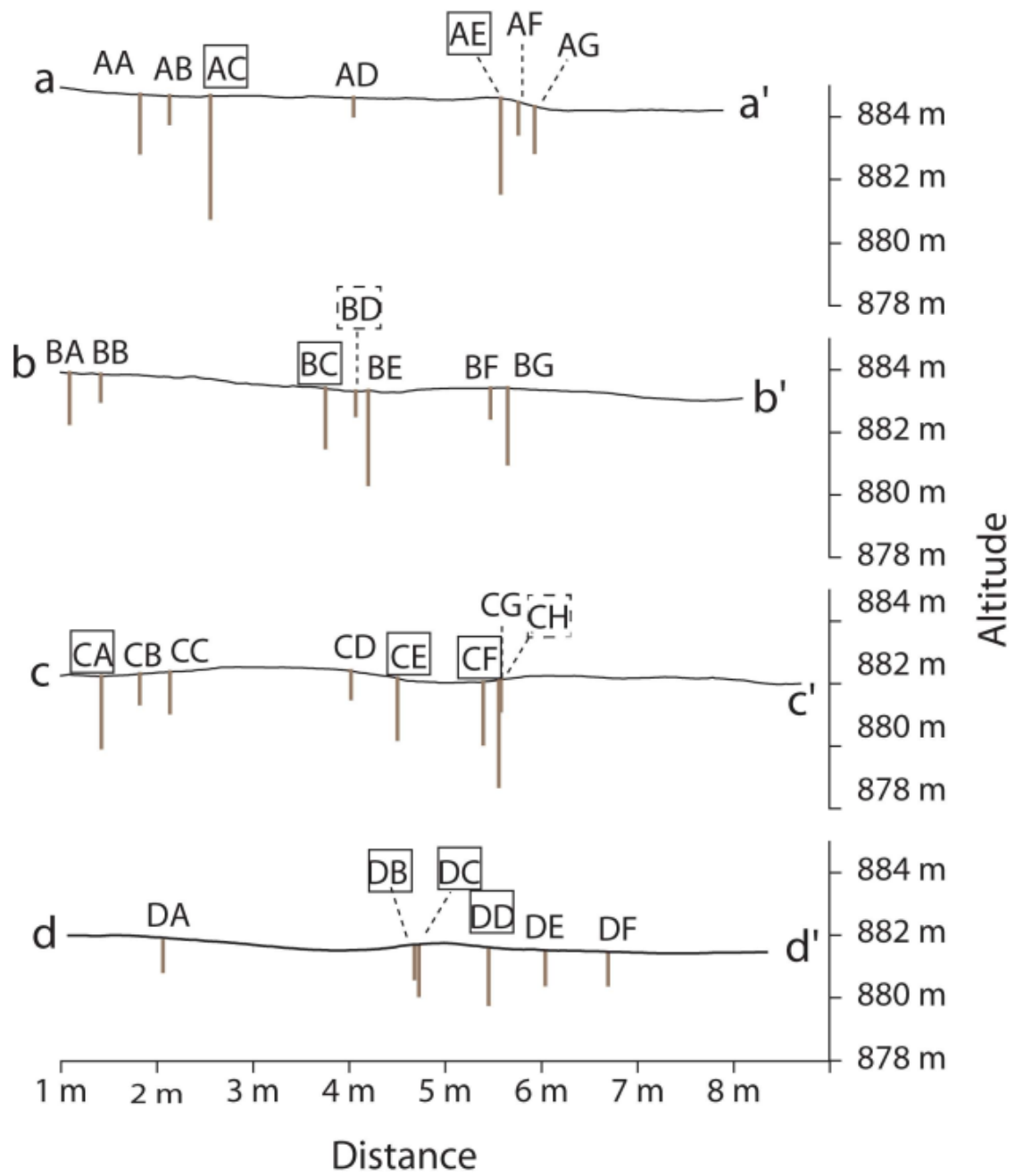
Soil profile showing the marl blocks layout and their different levels of weathering (blocks with stratification\flakes\fine matrix). The dashed arrows indicate the main direction of bedding.

FIGURE 3 :



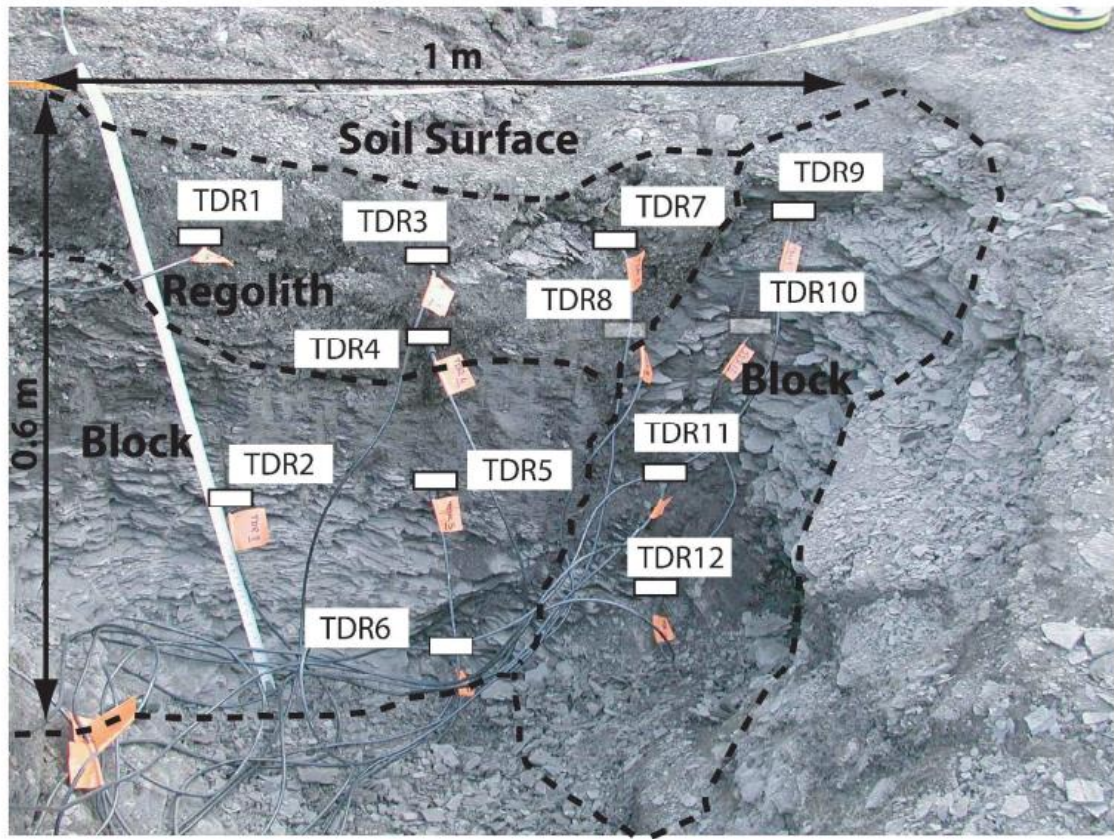
Layout of the experimental area. Depths and location of the observation wells according to 'aa'), 'bb'), (cc') or (dd') transects are shown on figure 4. Soil profile with TDR Trase probes is shown on figure 5

FIGURE 4:



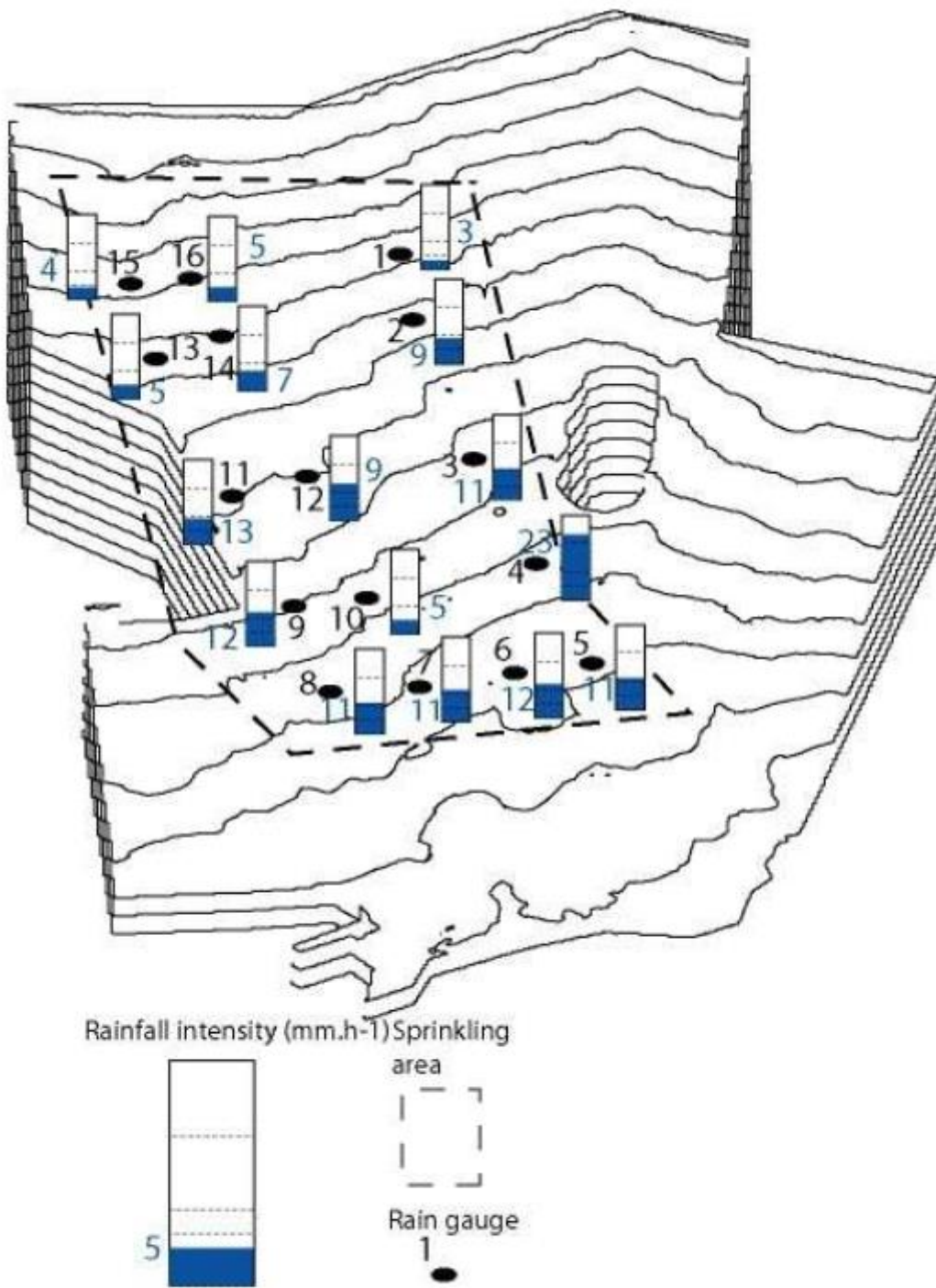
Location and depth of the observation wells along the (aa'), (bb'), (cc') and (dd') transects

FIGURE 5 :



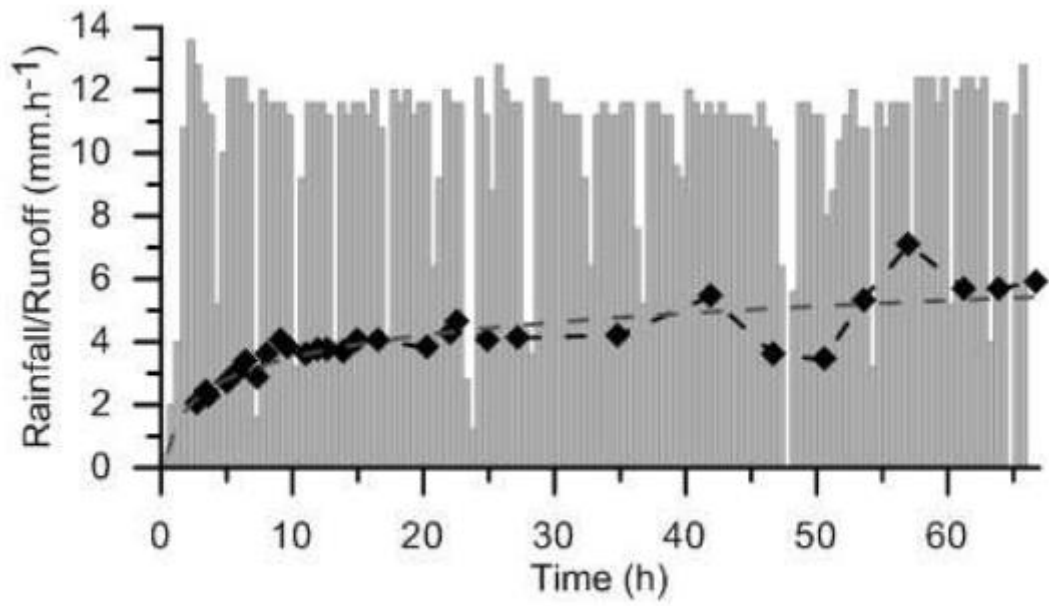
View of the soil moisture monitoring device. TDRs 1, 3, 4, 7 and 8 were inserted into the fine regolith. TDRs 2, 5, 6, 9, 10, 11 and 12 were inserted into marl blocks
1275x957mm (72 x 72 DPI)

FIGURE 6 :



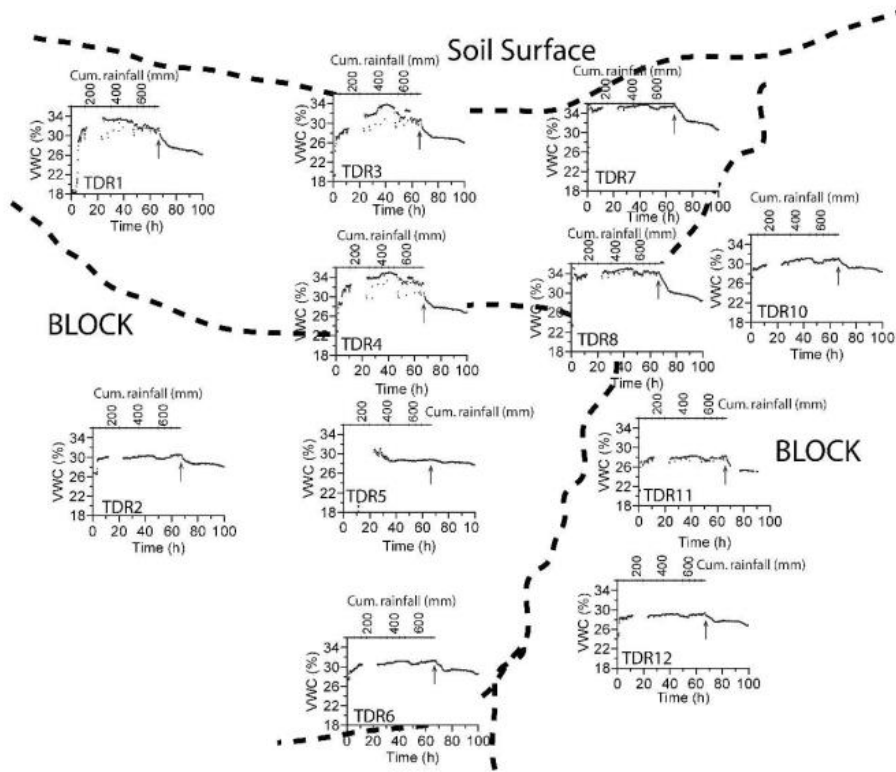
Average rainfall intensity over area during the experiment (mm.h⁻¹)
165x226mm (72 x 72 DPI)

FIGURE 7 :



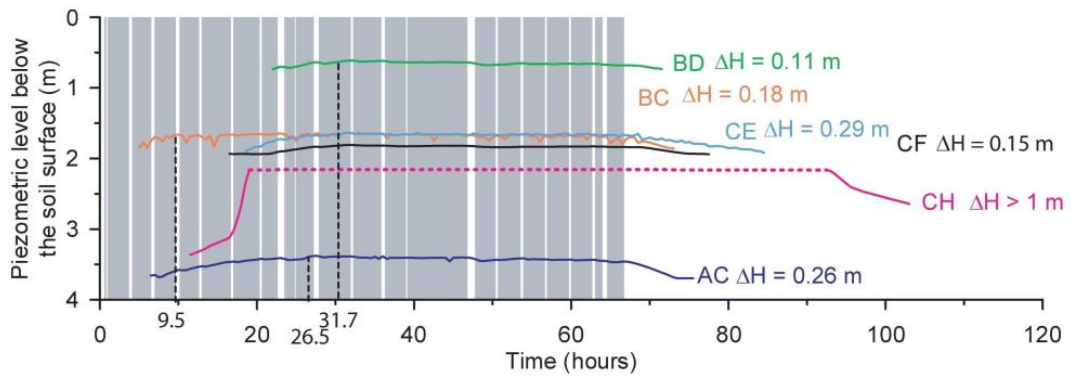
Variation over time of rainfall and surface runoff (in mm.h-1)
158x90mm (72 x 72 DPI)

FIGURE 8 :



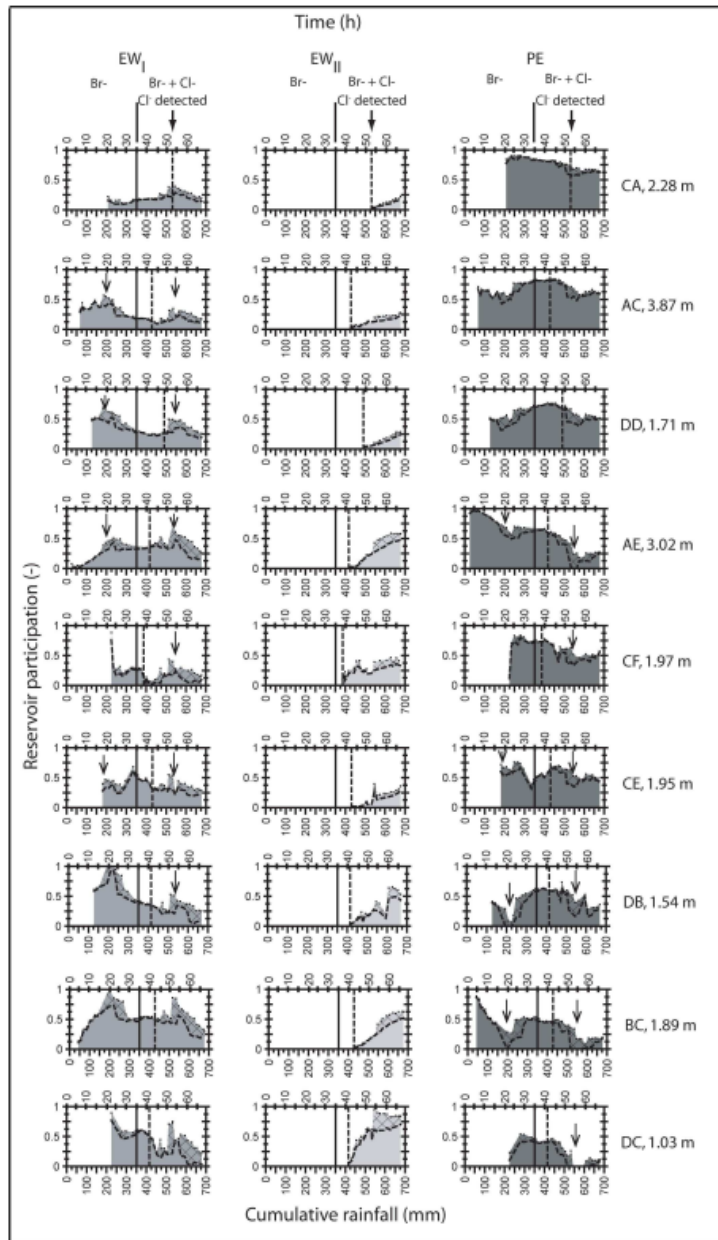
Volumetric water content in the regolith and marl blocks over the experiment
457x342mm (300 x 300 DPI)

FIGURE 9 :



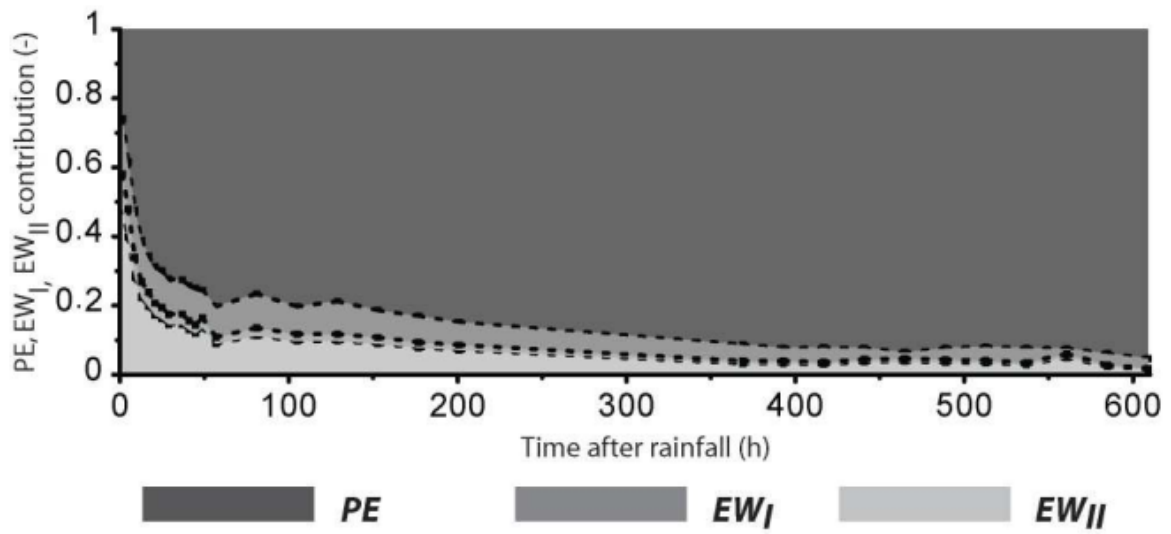
Water level variations in different piezometers during and after the rainfall simulation. The grey shaded areas indicate the sprinkling periods. ΔH gives the maximum level variations
935x323mm (72 x 72 DPI)

FIGURE 10 :



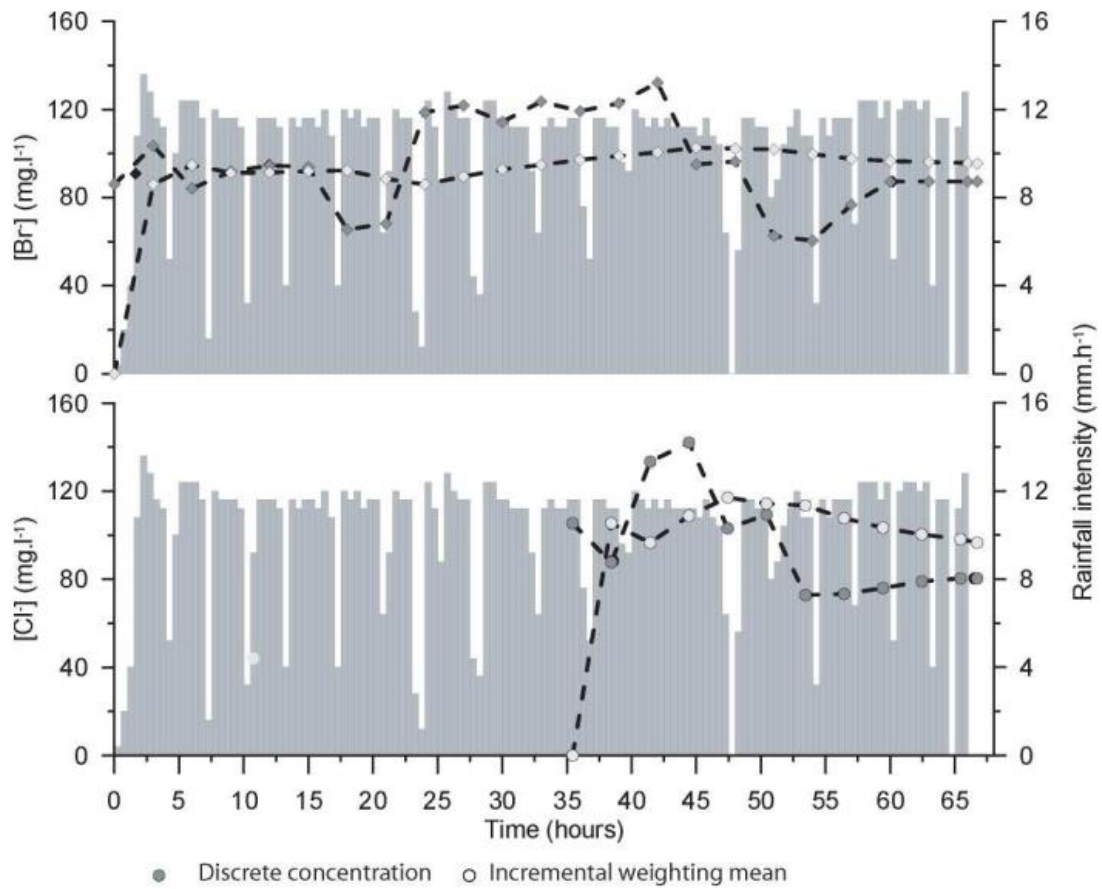
Contributions over time of PE (pre event water), EWI (event water phase I) and EWII (event water phase II) in different piezometers. The piezometers are sorted according to PE contributions (the larger contribution was in CA and the lower was in DC)
 180x310mm (300 x 300 DPI)

FIGURE 11 :



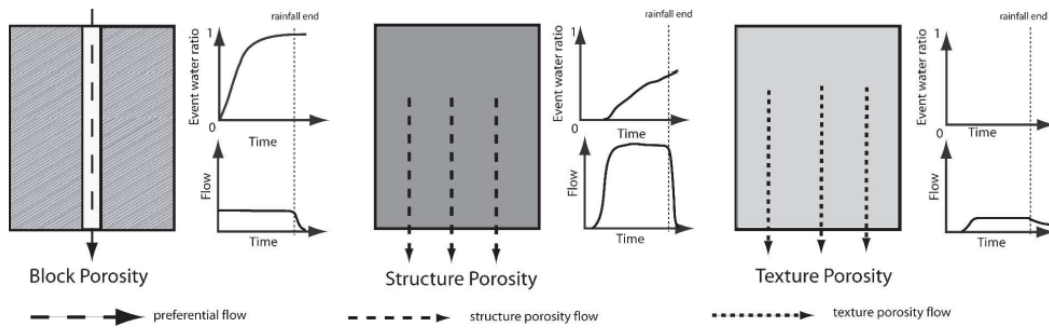
Variation of the components contribution during the recession phase in piezometer AE
350x161mm (72 x 72 DPI)

FIGURE 12 :



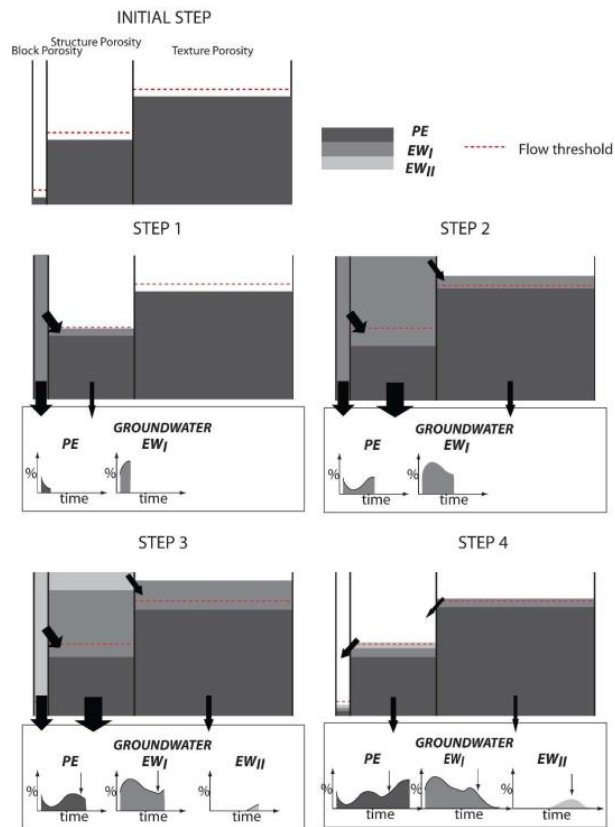
Variation in Br- and Cl- concentrations in event water during the experiment according to the weighting technique used. The grey shaded areas indicate the sprinkling periods
385x315mm (72 x 72 DPI)

FIGURE 13 :



Active porosities of the material and their impact on the shape of the hydrograph and event water contribution during and after a rainfall event
1356x409mm (72 x 72 DPI)

FIGURE 14 :



proposition of a stepwise conceptual model showing the role of reservoirs interactions on the hydrological dynamics
1582x1189mm (72 x 72 DPI)